

The CRAPome: a contaminant repository for affinity purification–mass spectrometry data

Dattatreya Mellacheruvu^{1,2}, Zachary Wright², Amber L Couzens³, Jean-Philippe Lambert³, Nicole A St-Denis³, Tuo Li⁴, Yana V Miteva⁴, Simon Hauri⁵, Mihaela E Sardiū⁶, Teck Yew Low^{7,8}, Vincentius A Halim^{7–9}, Richard D Bagshaw³, Nina C Hubner¹⁰, Abdallah al-Hakim³, Annie Bouchard¹¹, Denis Faubert¹¹, Damian Fermin¹, Wade H Dunham^{3,12}, Marilyn Goudreault³, Zhen-Yuan Lin³, Beatriz Gonzalez Badillo³, Tony Pawson^{3,12}, Daniel Durocher^{3,12}, Benoit Coulombe^{11,13}, Ruedi Aebersold^{5,14}, Giulio Superti-Furga¹⁵, Jacques Colinge¹⁵, Albert J R Heck^{7,8}, Hyungwon Choi¹⁶, Matthias Gstaiger⁵, Shabaz Mohammed^{7,8,17,18}, Ileana M Cristea⁴, Keiryn L Bennett¹⁵, Mike P Washburn^{6,19}, Brian Raught^{20,21}, Rob M Ewing^{22,23}, Anne-Claude Gingras^{3,12} & Alexey I Nesvizhskii^{1,2}

Affinity purification coupled with mass spectrometry (AP-MS) is a widely used approach for the identification of protein–protein interactions. However, for any given protein of interest, determining which of the identified polypeptides represent bona fide interactors versus those that are background contaminants (for example, proteins that interact with the solid-phase support, affinity reagent or epitope tag) is a challenging task. The standard approach is to identify nonspecific interactions using one or more negative-control purifications, but many small-scale AP-MS studies do not capture a complete, accurate background protein set when available controls are limited. Fortunately, negative controls are largely bait independent. Hence, aggregating negative controls from multiple AP-MS studies can increase coverage and improve the characterization of background associated with a given experimental protocol. Here we present the contaminant repository for affinity purification (the CRAPome) and describe its use for scoring protein–protein interactions. The repository (currently available for *Homo sapiens* and *Saccharomyces cerevisiae*) and computational tools are freely accessible at <http://www.crapome.org/>.

AP-MS has become a widely used approach for the identification of protein–protein interactions¹. In most cases, however,

a large number of nonspecific interactors (here referred to as ‘background contaminants’, or ‘contaminants’) are copurified with bait proteins and identified by mass spectrometry. Methods to discern bona fide interacting partners from background contaminants are thus essential. In the case of affinity purification using epitope-tagged proteins, this distinction is often aided by the inclusion of negative-control purifications, typically consisting of one or more mock purifications using the same support resin and cell line but without expression of the polypeptide(s) of interest (‘bait’ proteins). These controls (when isotope labeling^{2–5} is not used) can be considered universal, meaning that they are useful for filtering the background from any bait protein subjected to the same purification scheme^{3,6–10}.

A question that arises when designing and performing AP-MS experiments is how to use previous knowledge regarding background contaminants to best score interaction data. Small variations in the sample or sample preparation may influence the recovery of proteins, including contaminants. It is therefore not uncommon for a negative-control experiment to fail to capture a complete set of contaminants owing to undetected variations at one or more experimental steps. This issue is compounded by the fact that low-abundance peptides (and hence proteins) may not be reliably detected in a given mass spectrometry analysis. Analyzing

¹Department of Pathology, University of Michigan, Ann Arbor, Michigan, USA. ²Department of Computational Medicine and Bioinformatics, University of Michigan, Ann Arbor, Michigan, USA. ³Centre for Systems Biology, Samuel Lunenfeld Research Institute at Mount Sinai Hospital, Toronto, Ontario, Canada. ⁴Department of Molecular Biology, Princeton University, Princeton, New Jersey, USA. ⁵Department of Biology, Institute of Molecular Systems Biology, ETH Zurich, Zurich, Switzerland. ⁶Stowers Institute for Medical Research, Kansas City, Missouri, USA. ⁷Biomolecular Mass Spectrometry and Proteomics, Bijvoet Center for Biomolecular Research and Utrecht Institute for Pharmaceutical Sciences, Utrecht University, Utrecht, The Netherlands. ⁸Netherlands Proteomics Center, Utrecht, The Netherlands. ⁹Division of Cell Biology, Netherlands Cancer Institute, Amsterdam, The Netherlands. ¹⁰Department of Molecular Biology, Faculty of Science, Nijmegen Centre for Molecular Life Sciences, Radboud University, Nijmegen, The Netherlands. ¹¹Institut de Recherches Cliniques de Montréal, Montreal, Quebec, Canada. ¹²Department of Molecular Genetics, University of Toronto, Toronto, Ontario, Canada. ¹³Département de Biochimie, Université de Montréal, Montreal, Quebec, Canada. ¹⁴Faculty of Science, University of Zurich, Zurich, Switzerland. ¹⁵CeMM Research Center for Molecular Medicine of the Austrian Academy of Sciences, Vienna, Austria. ¹⁶Saw Swee Hock School of Public Health, National University of Singapore, Singapore. ¹⁷Department of Chemistry, University of Oxford, Oxford, UK. ¹⁸Department of Biochemistry, University of Oxford, Oxford, UK. ¹⁹Department of Pathology & Laboratory Medicine, University of Kansas Medical Center, Kansas City, Kansas, USA. ²⁰Ontario Cancer Institute, Toronto, Ontario, Canada. ²¹Department of Medical Biophysics, University of Toronto, Toronto, Ontario, Canada. ²²Center for Proteomics and Bioinformatics, Case Western Reserve University, Cleveland, Ohio, USA. ²³Present address: Centre for Biological Sciences, University of Southampton, Southampton, UK. Correspondence should be addressed to A.-C.G. (gingras@lunenfeld.ca) or A.I.N. (nesvi@med.umich.edu).

RECEIVED 9 JANUARY; ACCEPTED 18 MAY; PUBLISHED ONLINE 7 JULY 2013; DOI:10.1038/NMETH.2557

one or several negative-control samples will thus generally not allow for a comprehensive characterization of background contaminants for a given purification regime.

Here we present the CRAPome, a web-accessible resource that stores and annotates negative controls generated by the proteomics research community and enables their use for scoring AP-MS data. Users employ an intuitive graphical user interface to explore the database by either querying one protein at a time, downloading background contaminant lists for selected experimental conditions, or uploading their own data (alongside their own negative controls when available) and performing data analysis. We also describe database structure and composition, provide examples of the use of this resource to filter contaminants with properly chosen controls and demonstrate the utility of the scoring scheme for identifying bona fide interaction partners. The CRAPome accommodates a variety of purification schemes and, though it currently contains only *H. sapiens* and *S. cerevisiae* data, will be expanded to include other species.

RESULTS

Creation of the CRAPome repository

The CRAPome database is a web-accessible (<http://www.crapome.org/>) repository of negative-control AP-MS experiments (both published^{7,9-27} and unpublished) associated with detailed protocols and controlled vocabularies (CVs; **Supplementary Table 1**) used to organize the data. Data contributors first submit raw mass spectrometry files (**Fig. 1a** and **Supplementary Fig. 1**), which are processed using a uniform data analysis pipeline and by several quality-control checks (Online Methods) before the association of metadata (CVs and text-based protocols; **Supplementary**

Notes 1 and **2**). These annotated negative-control runs form the core of the repository. Currently (v.1.0, March 2013), 360 experiments contributed by 12 laboratories are available in the repository, of which the bulk of the data (343 experiments) were generated using human cell lines. This large data set covers many of the most commonly used AP-MS protocols (**Supplementary Table 1**; <http://www.crapome.org/>). For each experiment, mapping of the protein identifiers to the HUGO gene nomenclature committee (HGNC) gene symbol is performed, and spectral count information is parsed to the relational database (Online Methods). The database is expandable, and new data are added to the CRAPome using the same deposition and annotation process. New protocols and CVs will adapt the database to new experimental workflows.

Graphical user interface

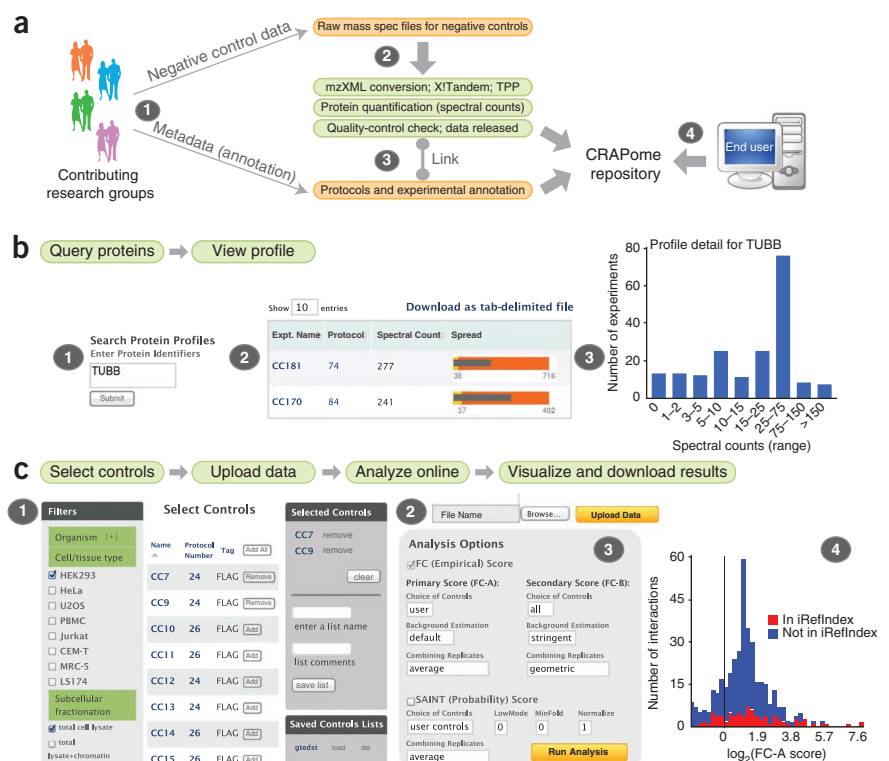
End users access the database via a web interface (**Fig. 1b,c** and **Supplementary Note 1**; <http://www.crapome.org/>). After selecting the organism of interest (currently *H. sapiens* or *S. cerevisiae*), the database can be queried in three ways (called “user workflows”).

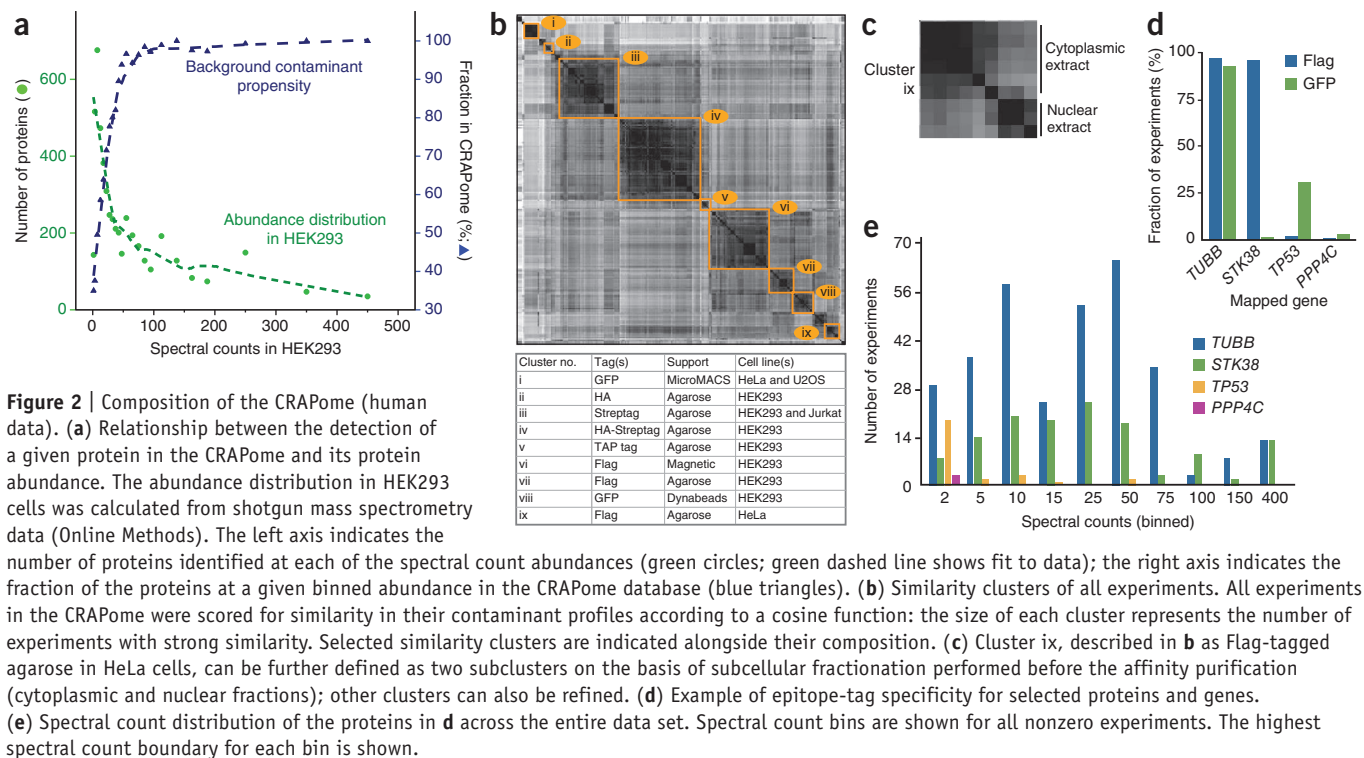
1. Query selected proteins. In workflow 1, users submit queries consisting of protein or gene identifiers and retrieve summaries of the occurrence of queried entries. An expanded view summarizes the conditions and protocols in which the protein has been identified, associated with spectral count information (**Fig. 1b**).

2. Create contaminant lists. Workflow 2 generates background lists from a subset of the CRAPome controls. In this case, the user simply selects the list of desired controls (filtered using CVs and protocol details; **Fig. 1c**) and downloads the resulting tables of contaminants. Quantitative parameters, including the occurrence

Figure 1 | The CRAPome at a glance.

(a) Creation of the CRAPome. (1) Contributors to the CRAPome submit raw mass spectrometry files for negative-control runs as well as detailed experimental protocols and mapping information. (2) Raw mass spectrometry files are first converted to mzXML and analyzed by X!Tandem and the Trans-Proteomic Pipeline (TPP); counts are extracted for protein quantification, and the CRAPome administrator performs a quality-control check (Online Methods). (3) Released high-quality runs (data) are associated with experimental descriptions and protocols (metadata) by the CRAPome administrator in consultation with the data provider. (4) The CRAPome database is queried by external users via the web interface. (b) Overview of the CRAPome workflow 1. (1) Proteins are queried against the CRAPome by inputting one of several identifiers (**Supplementary Note 1**), which are mapped to corresponding gene symbols. Different views enable exploration of the contaminant profile of each queried protein, either as a summary table (2) or in graphical formats (3). (c) Overview of the CRAPome workflow 3. (Note that workflow 2 is similar, except that no user data are uploaded; workflow 2 generates lists of contaminant proteins.) (1) Desired controls are selected, with the help of CVs. Users upload their own data (test experiments and controls if available) to the CRAPome (2) and select parameters for data analysis (3). Data are displayed in a tabular format and in different graphical formats; these visualizations include the detection of a given interaction in the public repository iRefIndex (4).





of identification across selected controls and the average spectral counts across selected controls in which the protein was detected, are included (a maximum of 30 experiments can be viewed online and included for analysis in workflow 3 below; the entire data set can be downloaded as a tab-delimited file from <http://www.crapome.org/>). Registered users can also save the selected list of controls for future use.

3. Analyze user data. Workflow 3 allows users to analyze their own data, using selected CRAPome controls and/or their own controls. The input data consist of one or multiple AP-MS experiments, ideally including biological replicates, along with user controls (optional, but recommended for better discrimination of true interactors from contaminants). Preparation of the data for upload to the CRAPome is described in Online Methods. In a first step, the user selects relevant controls from the CRAPome database (using the same interface as for workflow 2; Fig. 1c) or chooses previously saved selected lists of controls. The user then uploads data in the specified format (or uses previously uploaded data). Upon selection of baits and controls, analysis is performed with the significance analysis of interactome (SAINT) score^{28–30} and/or a simpler fold-change (FC) calculation (detailed below). These scoring tools create lists of interacting partners ranked by confidence. Previously reported interactions documented in the interaction database aggregator iRefIndex (v.9.0; ref. 31) are also mapped onto user data. The results are presented in a tabular format and can be downloaded as a tab-delimited file. Additionally, summary graphical views of the data are provided for each bait protein (Fig. 1c) or for all baits combined, enabling the user to view their data at a glance.

Characterization of the CRAPome

We mined the database to determine (i) which proteins have a higher propensity to be contaminants and (ii) how background

proteins differ according to experimental conditions. First, to understand whether the abundance level of a protein in a sample increases the propensity of the protein to be a contaminant, we plotted the proteins reported in the CRAPome repository (restricting the analysis to HEK293 cells, by far the most common human cell line in the CRAPome) against a list of proteins ranked by their abundance estimates on the basis of whole-proteome analysis of HEK293 cell lysate³². We observed a clear relationship between the abundance of a protein in HEK293 and its detection in at least one of the HEK293 experiments in the CRAPome (Fig. 2a). We next analyzed the frequency of detection of individual proteins in the CRAPome (mapped to gene names, as throughout this manuscript). Using stringent filtering (protein false discovery rate <1%), 4,449 nonredundant protein groups (or 7,782 gene names without compression of the data; Online Methods) were identified (see **Supplementary Tables 2 and 3** for the most frequently detected proteins and the “Supplementary Data” section of <http://www.crapome.org/> for complete lists). Of these, 14 proteins were detected in >90% of all experiments, and 89 were detected in >50% of the experiments: percentages that qualified these proteins as ubiquitous contaminants (Table 1). These include keratins, cytoskeletal proteins such as tubulins and actins, and high-abundance proteins including translation elongation factors and histones (Table 2). Other proteins were not detected consistently across all purifications but were abundant (in terms of total spectral counts) across the database: these were notably enriched for several functional categories, predominantly those associated with RNA functions (Supplementary Tables 4–6). However, a large fraction of the proteins present in the CRAPome were detected in only a small fraction of experiments: 3,571, or 80% of the proteins in the CRAPome, were found in ≤10% of the experiments.

Table 1 | Frequency of detection across the CRAPome

Frequency in CRAPome (%)	Redundant gene counts	Reduced gene counts
>90	15	14
>75	37	30
>50	110	89
>20	504	463
>10	898	878
≤10	6,884	3,571
Total	7,782	4,449

Data are for *H. sapiens*. The two counts are computed at different frequencies. (i) "Redundant" gene counts are based on a generous estimation of shared peptides: in this case, each protein or gene to which a given peptide is matched is counted as a contaminant. (ii) "Reduced" gene counts are based on a more stringent definition of protein/gene parsimony, as described in the Online Methods.

To further explore the contaminant propensity of the proteins in the CRAPome, we computed the similarity of all experiments (restricting the analysis to human data only), generating a heat map (Fig. 2b and Online Methods). The data clustered primarily according to experimental conditions (though there was a bias in the type of background detected across different laboratories). Several of the clusters could be further separated into subclusters, as exemplified by the "Flag HeLa agarose" cluster, which showed a clear separation based on subcellular fractionation (cytoplasmic or nuclear) performed before AP-MS (Fig. 2c). Using our analysis of the most important determinants of background behavior as a basis, we annotated all experiments in the CRAPome using 14 categories of CVs (Supplementary Table 1), which can be used to select experiments that are most similar to those in a query set. Complete protocol descriptions of the experiments are also provided by selecting the desired protocol number.

To illustrate the different contaminant propensities of individual proteins, and the need to account for not only the overall frequency of detection in the data set but also the experimental conditions, we analyzed the frequency distribution of four proteins with two types of epitope tags, Flag and GFP (Fig. 2d). Tubulin- β (TUBB) was detected across nearly all of the experiments, irrespective of the epitope tag. By contrast, the serine/threonine kinase STK38 copurified in nearly all Flag experiments but not in GFP experiments, whereas the tumor suppressor protein p53 (TP53) was detected predominantly in GFP-based affinity purification protocols. The serine/threonine phosphatase PPP4C was not detected at a high frequency in experiments performed with either of these epitope tags (it was identified in 3 of 343 experiments across the entire database). Frequency and experimental conditions are also clearly insufficient to describe contaminant propensity: abundance measures are also critical. For instance, if a protein is detected at a high frequency but low abundance (that is, a low number of spectral counts in a high number of mass spectrometry runs) in the CRAPome but is detected with a high spectral count in bait purifications performed by a user, it is more likely to be a true interactor than if it were always detected with high abundance in the CRAPome. To illustrate this concept, we compared the nonzero values in Figure 2d for the four proteins, but we specifically examined spectral count distributions (binned values). This analysis revealed that whereas TUBB and STK38 were often present in very high counts in the CRAPome, TP53 was usually detected with much lower spectral counts (Fig. 2e). Such comparisons can be easily accessed via the CRAPome user interface

(Supplementary Note 1). They also provide the basis for statistical or empirical scoring of interactions, as described below.

Using the CRAPome to score interactions

The CRAPome can be used for the analysis of diverse AP-MS data sets and, most importantly, for relatively small data sets, for which eliminating background contaminants computationally is a difficult task. The CRAPome implements two complementary scoring strategies, both based on quantitative comparisons of abundance levels (estimated using spectral counts) of coprecipitating proteins (prey) in purifications with bait proteins against the distribution of prey abundances across a set of negative controls (Online Methods). SAINT, described previously^{10,28–30}, allows advanced statistical modeling of the input bait-prey spectral count data and reports a posterior probability of true interaction. A simpler FC calculation is based on the ratio of average normalized spectral counts in bait purifications to negative controls. FC scoring is customizable and, in addition to the calculation of the standard FC score (referred to as primary score, or FC-A), involves the computation of a secondary, more stringent score (FC-B; see below). Both FC and SAINT calculations are run in parallel using the CRAPome interface (allowing specification of key model parameters³⁰), and comparison of their relative performances for each of the tested baits can be assessed by a receiver operating characteristic (ROC) analysis provided via the CRAPome interface.

The use of the analytical pipeline within the CRAPome is illustrated here by a small data set consisting of two biological replicates of each of the following four baits: RAF1, EIF4A2, WASL and MEPCE. In addition, six matching controls (user controls) were generated and processed together with the four baits to generate the input data (Online Methods). MEPCE and EIF4A2 have many documented interactors³¹, whereas WASL and RAF1 have fewer known interactors; all proteins provide challenges for background definition because of their association with polypeptides with contaminant-like behavior (chaperones, cytoskeletal proteins, RNA-binding proteins and so on; Table 2).

We first evaluated the results by plotting ROC curves based on the information extracted from iRefIndex³¹. The protein interaction list (all four baits combined) was sorted on the basis of either the SAINT probability or the FC-A score computed using the six user controls (Fig. 3a). Although SAINT outperformed the FC-A score on this data set, both scoring schemes were able to efficiently recapitulate known interactions from the literature. Both scores also tracked very similarly for most of the proteins analyzed (Fig. 3b), with SAINT essentially providing a statistical conversion of the FC onto the probability scale via the

Table 2 | Most frequently detected protein families across the CRAPome

Gene family	Example gene symbols
Heat-shock proteins	<i>HSPA1A, HSPA8, HSPA2</i>
Keratins	<i>KRT1, KRT10, KRT2</i>
Tubulins	<i>TUBA1B, TUBA3C, TUBB</i>
Actins	<i>ACTB, ACTA2, ACTBL2</i>
Elongation factors	<i>EEF1A, EEF1A2</i>
Histones	<i>HIST1H1C, H2AFX, HIST2H2BE</i>
Ribonucleoproteins	<i>HNRNPK, HNRNPU, HNRNPH1</i>
Ribosomal proteins	<i>RPS3, RPS18, RPL23</i>

Shown are the most frequently detected protein families, alongside some of the most frequently detected representative genes (*H. sapiens* data).

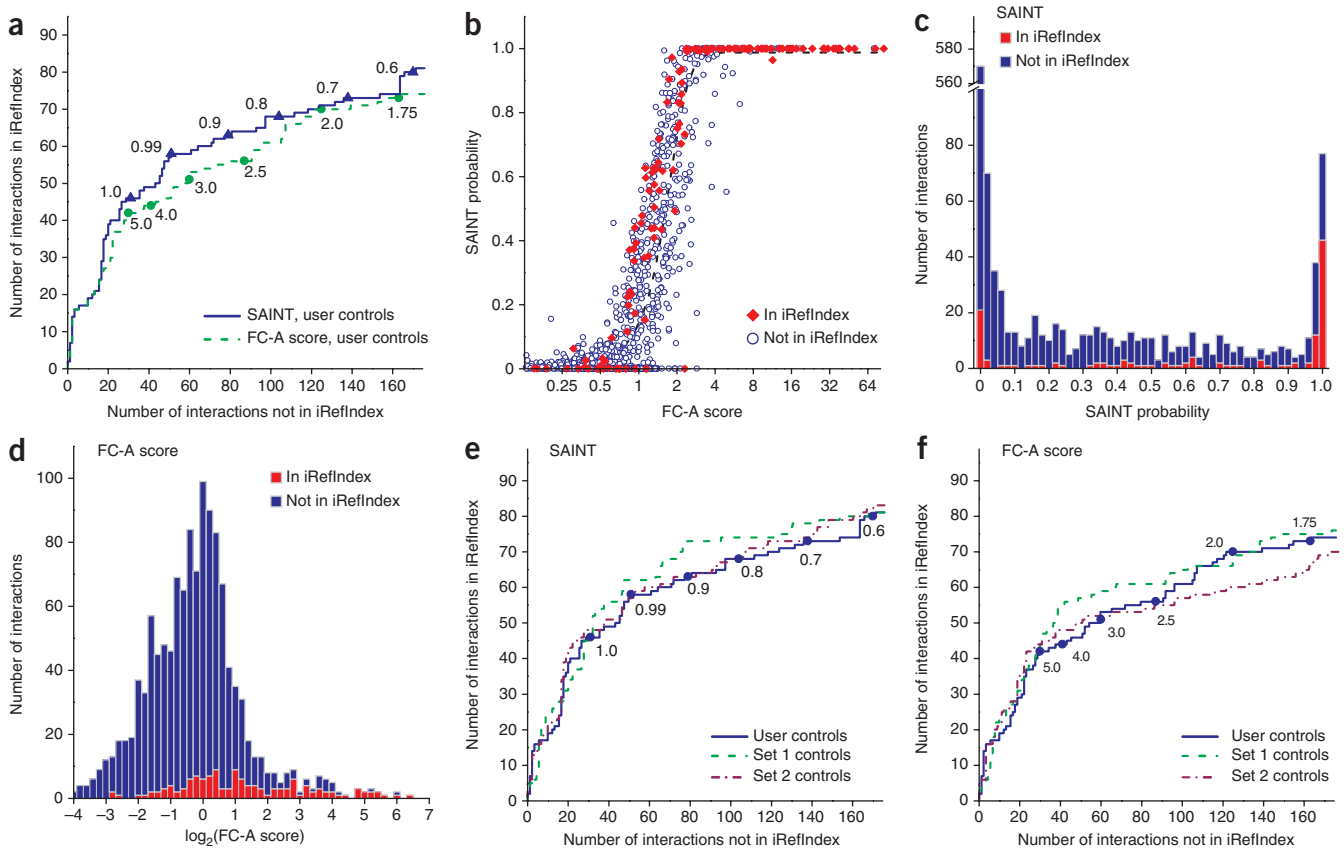


Figure 3 | Scoring functions in the CRAPome illustrated on a four-bait data set (MEPCE, EIF4A2, WASL and RAF1; eight experiments). **(a)** Comparison between the FC-A score and SAINT for scoring known interactions using negative-control runs ($n = 6$) provided by the user; the receiver operating characteristic is based on the interactions in iRefIndex. Note that when SAINT scores are identical, ties are broken by the FC-A score. Selected SAINT probability or FC-A score thresholds are represented by triangles and circles, respectively. **(b)** The relationship between SAINT probability and FC score is well represented by a sigmoid function (dashed curve). **(c, d)** Histogram visualization of the data presented in **b** can help with data exploration and threshold selection. **(e, f)** Scoring protein interactions using controls from the CRAPome with SAINT **(e)** and FC-A **(f)**: user controls ($n = 6$) are compared to two sets of controls from the CRAPome, selected according to the CVs (set 1 = 10 controls; set 2 = 11 controls).

mixture-model analysis of the underlying spectral count distributions. We further visualized the performance of the interaction scores by plotting the distribution of scores (histograms) separately on the basis of iRefIndex annotation, which showed that high-scoring interactions (SAINT probability above 0.9, FC score above 4) are clearly enriched for previously reported interactions (Fig. 3c,d). The CRAPome interface provides (both separately for each analyzed bait and for all baits combined) an ROC and a histogram view (with mouse-over function), which enables the user to explore the reported interactions at different scores for SAINT or FC and assists in establishing appropriate thresholds.

We next tested whether the controls deposited in the CRAPome could be used for scoring interactions in the absence of user controls. Although we recommend always using at least some user controls for scoring interactions, there are certainly cases in which such controls do not appropriately model the background. Controls from the repository were thus selected on the basis of the CVs and protocols. We identified two relevant control sets from two different laboratories that fulfilled our criteria (HEK293 cells, Flag tag, single-step purification on M2 agarose) which contained 10 (set 1; CRAPome protocol no. 56) and 11 (set 2; CRAPome protocol no. 26) experiments, respectively. Using ROC analysis, we showed that each of these sets of

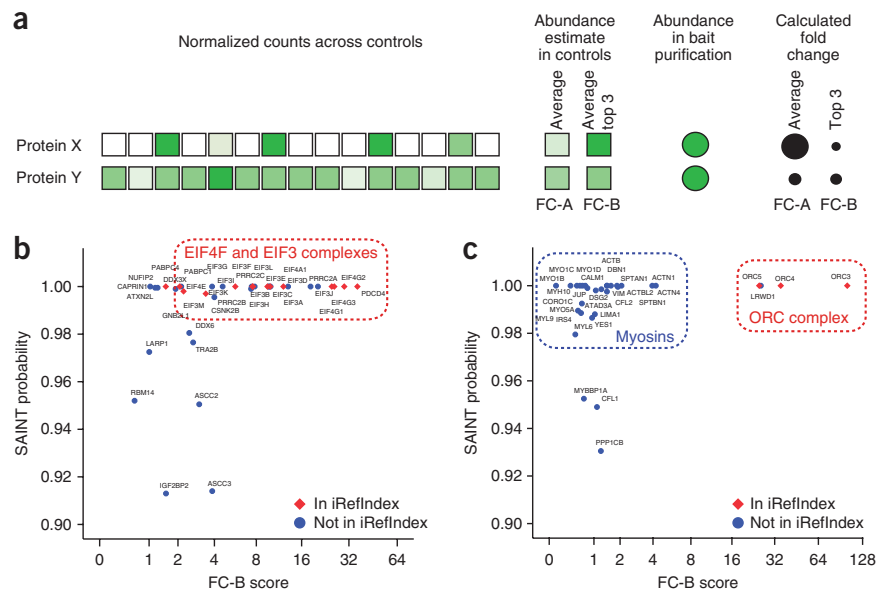
controls performed very similarly to the user controls in both SAINT (Fig. 3e) and FC (Fig. 3f) calculations.

One issue affecting the scoring of AP-MS data is the existence of contaminants (for example, myosin and the proteins that copurify with it) that are usually present in small amounts across most controls but that can spike to high abundance in some controls (or across batches of purifications), making detection of the true interactors much more difficult. Such contaminants are normally ‘diluted out’ when multiple experiments are used for FC calculation, or even SAINT analysis (Fig. 4a). To assist in the identification of these ‘rare’ contaminants, we implemented a more conservative FC score, FC-B, that is automatically calculated to supplement normal scoring using SAINT or the FC-A score (Online Methods and Fig. 4a). We applied this more stringent scoring scheme to two biological replicates of the bait ORC2L, which, through visual inspection of the results, we found to contain large quantities of myosin contamination. Although SAINT is capable of identifying true interactors in successful experiments, as exemplified by EIF4A2 (Fig. 4b; note the relatively good agreement between the SAINT score and FC-B score), it assigned a high probability to myosins and associated proteins in the ORC2L samples (Fig. 4c). By contrast, the FC-B scores readily distinguished between these contaminants and true interaction partners

Figure 4 | Use of the FC-B score to recover true interacting partners for ORC2L.

(a) Illustration of the consequences of averaging all spectral counts instead of selecting the top three maximal values for scoring protein-protein interactions. Protein X represents a contaminant in the purification scheme that is detected with variable counts across the 15 selected controls (the intensity of shading is proportional to the spectral counts). By contrast, protein Y is a contaminant detected with similar counts across all selected controls. The FC-A calculation averages the counts across all controls, whereas the more stringent FC-B score takes the average of the top three highest spectral counts for the abundance estimate. The resulting FC-A and FC-B scores are represented schematically, where a larger circle indicates a higher fold change, with FC-A and FC-B assigning a similar score to protein Y but not to protein X.

(b) Comparison of SAINT–FC-B scoring with good bait samples. Note that only the top of the map (the interactions with SAINT probability ≥ 0.9) are displayed. (c) Same as **b** for bait samples (ORC2L) contaminated with myosin: the more stringent fold-change score FC-B helps in discriminating between true interaction partners (labeled “ORC complex”) and contaminants (labeled “myosins”).



(ORC3, ORC4 and ORC5 are in iRefIndex³¹, and LRWD1 is reported in PubMed³³). Notably, the CRAPome interface enables rapid visualization of the samples likely affected by this type of low-frequency contaminants by providing comparisons between FC-B and SAINT or FC-A.

DISCUSSION

Although lists of contaminating proteins have been reported in the past^{3,34,35}, there has been no central repository for this type of data or freely available software tools for using these lists. The CRAPome facilitates access to a standardized (in terms of protein identification pipeline, ID mapping, abundance measures and so on) set of negative-control experiments, organized via CVs based on experimental considerations. The freely accessible user interface is intuitive and informative, even for those who may be new to mass spectrometry.

We are currently using spectral counts as the sole quantification tool in the repository, but extension of the system to other types of quantification (especially that based on peptide ion intensity, which is becoming possible as high–mass resolution instruments are increasingly being used for AP-MS experiments) may help to further discriminate between background contaminants and true interactors. We expect a constant stream of negative-control data to be deposited in the CRAPome. Although we have restricted the release of the first version of the CRAPome to *H. sapiens* and *S. cerevisiae* data, the system is ready to accommodate data from other species, which will further increase the usefulness of the system. As contributors continue depositing their data in the repository, robustness in scoring will increase, and in-depth characterization of contaminant behavior will be possible. The CRAPome can be used as a retrospective tool to analyze AP-MS data, and it will be instrumental to curators of protein-protein interaction databases. It should also assist with establishing guidelines regarding the scoring and annotation of such data.

Widespread adoption of the CRAPome (by experimentalists, computational biologists, database curators and reviewers alike) will improve the overall quality of AP-MS protein interaction data, addressing one of the key challenges in proteomics research.

METHODS

Methods and any associated references are available in the [online version of the paper](#).

Note: Supplementary information is available in the [online version of the paper](#).

ACKNOWLEDGMENTS

We wish to thank G.I. Chen, M. Mullin, M.J. Kean, T.M. Greco, T. Srikumar and Y.-C. Tsai for contributing published data and S. Saha and J.-E. Dazard for constructive comments. We thank A. Stefanovic, M. Planyavsky, A. Stukalov, A.J. Guise, A.C. Müller, A. Pichlmair, B. Larsen, C. Knoll, C.L. Baumann, E.L. Rudashevskaya, F. Grebien, F.P. Breitwieser, H.G. Budayeva, J.W. Bigenzahn, M. Bruckner, M. Licciardello, M.L. Huber, M. Tucholska, N. Venturini, O. Rocks, O. Stein, P. Joshi, R. Giamb Bruno, R. Sacco, S. Zhang, T. Stasyk and V. Nguyen for help with sample analysis.

This work was supported by grants from the US National Institutes of Health (NIH 5R01GM94231 to A.-C.G. and A.I.N.; DP1DA026192 and HL112618-01 to I.M.C.), the Canadian Institutes of Health Research (CIHR MOP-84314 to A.-C.G.; MOP-82851 to B.C.), the government of Ontario via a Global Leadership Round in Genomics and Life Sciences (T.P. and A.-C.G.), the Austrian Academy of Sciences (K.L.B., J.C. and G.S.-F.), the Austrian Federal Ministry for Science and Research (Gen-Au projects, APP-III and BIN-III; K.L.B. and G.S.-F., no. 820965; J.C. and K.L.B., no. 820962), the European Research Council (G.S.-F.; ERC-2009-AdG-250179-i-FIVE), the Austrian Science Fund FWF (G.S.-F., J.C. and K.L.B.; P24321-B21 and P22282-B11), the European Molecular Biology Organization long-term fellowship (G.S.-F., J.C. and K.L.B.; ATLF463-2008), The Netherlands Proteomics Center (T.Y.L., V.A.H., S.M. and A.J.R.H.), the European Union 7th Framework Program (PRIME-XS project, grant no. 262067; T.Y.L., V.A.H., S.M., R.A. and A.J.R.H.), the Stowers Institute for Medical Research, and the Human Frontier Science Program (RGY0079/2009-C to I.M.C.). A.-C.G. is the Canada Research Chair in Functional Proteomics and the Lea Reichmann Chair in Cancer Proteomics; B.R. is the Canada Research Chair in Proteomics and Molecular Medicine. R.M.E. acknowledges salary support from the Cleveland Foundation and NIH 1R21 CA16006001A1. J.-P.L. and R.D.B. were supported by CIHR postdoctoral awards. N.A.S.-D. was supported by a TD Bank postdoctoral fellowship.

AUTHOR CONTRIBUTIONS

D.M., Z.W., A.I.N. and A.-C.G. designed the CRAPome structure and interface; D.M. and Z.W. implemented the system; D.M. and A.I.N. created the scoring scheme with help from H.C. and A.-C.G.; R.M.E., A.-C.G. and A.I.N. initiated the project; D. Fermin helped with processing the data; B.R., A.L.C., N.A.S.-D. and J.-P.L. tested the interface and contributed to editing the user manuals; A.L.C., N.A.S.-D., J.-P.L., W.H.D., T.L., Y.V.M., S.H., M.E.S., T.Y.L., V.A.H., R.D.B., N.C.H., A.a.-H., A.B., D. Faubert, R.M.E., I.M.C., K.L.B. and A.-C.G. provided mass spectrometry data to the CRAPome and/or annotated data in the repository; Z.-Y.L., B.G.B. and M. Goudreault contributed the test benchmark data set; T.P., D.D., B.C., R.A., G.S.-F., J.C., A.J.R.H., M. Gstaiger, S.M., I.M.C., K.L.B., M.P.W. and A.-C.G. supervised trainees and were responsible for data generation across the different research groups; H.C., B.R., I.M.C., K.L.B., M.P.W. and R.M.E. provided critical comments throughout the project; A.-C.G. and A.I.N. codirected the project and analyzed and annotated data; A.I.N., A.-C.G. and D.M. wrote the manuscript and the user manuals with help from B.R.

COMPETING FINANCIAL INTERESTS

The authors declare no competing financial interests.

Reprints and permissions information is available online at <http://www.nature.com/reprints/index.html>.

1. Gingras, A.C., Gstaiger, M., Raught, B. & Aebersold, R. Analysis of protein complexes using mass spectrometry. *Nat. Rev. Mol. Cell Biol.* **8**, 645–654 (2007).
2. Selbach, M. & Mann, M. Protein interaction screening by quantitative immunoprecipitation combined with knockdown (QUICK). *Nat. Methods* **3**, 981–983 (2006).
3. Trinkle-Mulcahy, L. *et al.* Identifying specific protein interaction partners using quantitative mass spectrometry and bead proteomes. *J. Cell Biol.* **183**, 223–239 (2008).
4. Trinkle-Mulcahy, L. Resolving protein interactions and complexes by affinity purification followed by label-based quantitative mass spectrometry. *Proteomics* **12**, 1623–1638 (2012).
5. Tackett, A.J. *et al.* I-DIRT, a general method for distinguishing between specific and nonspecific protein interactions. *J. Proteome Res.* **4**, 1752–1756 (2005).
6. Dunham, W.H., Mullin, M. & Gingras, A.C. Affinity-purification coupled to mass spectrometry: basic principles and strategies. *Proteomics* **12**, 1576–1590 (2012).
7. Hubner, N.C. *et al.* Quantitative proteomics combined with BAC TransgeneOmics reveals *in vivo* protein interactions. *J. Cell Biol.* **189**, 739–754 (2010).
8. Nesvizhskii, A.I. Computational and informatics strategies for identification of specific protein interaction partners in affinity purification mass spectrometry experiments. *Proteomics* **12**, 1639–1655 (2012).
9. Sardi, M.E. *et al.* Probabilistic assembly of human protein interaction networks from label-free quantitative proteomics. *Proc. Natl. Acad. Sci. USA* **105**, 1454–1459 (2008).
10. Skarra, D.V. *et al.* Label-free quantitative proteomics and SAINT analysis enable interactome mapping for the human Ser/Thr protein phosphatase 5. *Proteomics* **11**, 1508–1516 (2011).
11. Al-Hakim, A.K., Bashkurov, M., Gingras, A.C., Durocher, D. & Pelletier, L. Interaction proteomics identify NEURL4 and the HECT E3 ligase HERC2 as novel modulators of centrosome architecture. *Mol. Cell. Proteomics* **11**, M111.014233 (2012).
12. Chen, G.I. *et al.* PP4R4/KIAA1622 forms a novel stable cytosolic complex with phosphoprotein phosphatase 4. *J. Biol. Chem.* **283**, 29273–29284 (2008).
13. Cristea, I.M., Williams, R., Chait, B.T. & Rout, M.P. Fluorescent proteins as proteomic probes. *Mol. Cell. Proteomics* **4**, 1933–1941 (2005).
14. Daniels, D.L. *et al.* Examining the complexity of human RNA polymerase complexes using HaloTag technology coupled to label free quantitative proteomics. *J. Proteome Res.* **11**, 564–575 (2012).
15. Dunham, W.H. *et al.* A cost-benefit analysis of multidimensional fractionation of affinity purification-mass spectrometry samples. *Proteomics* **11**, 2603–2612 (2011).
16. Ewing, R.M. *et al.* Large-scale mapping of human protein-protein interactions by mass spectrometry. *Mol. Syst. Biol.* **3**, 89 (2007).
17. Forget, D. *et al.* The protein interaction network of the human transcription machinery reveals a role for the conserved GTPase RPAP4/GPN1 and microtubule assembly in nuclear import and biogenesis of RNA polymerase II. *Mol. Cell. Proteomics* **9**, 2827–2839 (2010).
18. Goudreault, M. *et al.* A PP2A phosphatase high density interaction network identifies a novel striatin-interacting phosphatase and kinase complex linked to the cerebral cavernous malformation 3 (CCM3) protein. *Mol. Cell. Proteomics* **8**, 157–171 (2009).
19. Kean, M.J. *et al.* Structure-function analysis of core STRIPAK proteins: a signaling complex implicated in Golgi polarization. *J. Biol. Chem.* **286**, 25065–25075 (2011).
20. Kruiswijk, F. *et al.* Coupled activation and degradation of eEF2K regulates protein synthesis in response to genotoxic stress. *Sci. Signal.* **5**, ra40 (2012).
21. Sato, S. *et al.* A set of consensus mammalian mediator subunits identified by multidimensional protein identification technology. *Mol. Cell* **14**, 685–691 (2004).
22. de Lau, W. *et al.* Lgr5 homologues associate with Wnt receptors and mediate R-spondin signalling. *Nature* **476**, 293–297 (2011).
23. Greco, T.M., Yu, F., Guise, A.J. & Cristea, I.M. Nuclear import of histone deacetylase 5 by requisite nuclear localization signal phosphorylation. *Mol. Cell. Proteomics* **10**, M110.004317 (2011).
24. Tsai, Y.C., Greco, T.M., Boonmee, A., Miteva, Y. & Cristea, I.M. Functional proteomics establishes the interaction of SIRT7 with chromatin remodeling complexes and expands its role in regulation of RNA polymerase I transcription. *Mol. Cell. Proteomics* **11**, M111.015156 (2012).
25. Rudashevskaya, E.L. *et al.* A method to resolve the composition of heterogeneous affinity-purified protein complexes assembled around a common protein by chemical cross-linking, gel electrophoresis and mass spectrometry. *Nat. Protoc.* **8**, 75–97 (2013).
26. Pichlmair, A. *et al.* Viral immune modulators perturb the human molecular network by common and unique strategies. *Nature* **487**, 486–490 (2012).
27. Varjosalo, M. *et al.* Interlaboratory reproducibility of large-scale human protein-complex analysis by standardized AP-MS. *Nat. Methods* **10**, 307–314 (2013).
28. Breitkreutz, A. *et al.* A global protein kinase and phosphatase interaction network in yeast. *Science* **328**, 1043–1046 (2010).
29. Choi, H. *et al.* SAINT: probabilistic scoring of affinity purification-mass spectrometry data. *Nat. Methods* **8**, 70–73 (2011).
30. Choi, H. *et al.* Analyzing protein-protein interactions from affinity purification-mass spectrometry data with SAINT. *Curr. Protoc. Bioinformatics* **39**, 8.15 (2012).
31. Razick, S., Magklaras, G. & Donaldson, I.M. iRefIndex: a consolidated protein interaction database with provenance. *BMC Bioinformatics* **9**, 405 (2008).
32. Thakur, S.S. *et al.* Deep and highly sensitive proteome coverage by LC-MS/MS without prefractionation. *Mol. Cell. Proteomics* **10**, M110.003699 (2011).
33. Shen, Z. *et al.* A WD-repeat protein stabilizes ORC binding to chromatin. *Mol. Cell* **40**, 99–111 (2010).
34. Chen, G.I. & Gingras, A.C. Affinity-purification mass spectrometry (AP-MS) of serine/threonine phosphatases. *Methods* **42**, 298–305 (2007).
35. Gingras, A.C. *et al.* A novel, evolutionarily conserved protein phosphatase complex involved in cisplatin sensitivity. *Mol. Cell. Proteomics* **4**, 1725–1740 (2005).



ONLINE METHODS

Design and architecture of the CRAPome. The CRAPome interface was developed using Drupal, an open-source PHP-based web framework, and MySQL and SQLite relational databases. The processing pipeline for adding data to the database, processing user input data, extracting data from the database, computing FC scores, and preparing summary reports was developed using Python and a SQLite database. SAINT analysis^{29,30} is computationally intensive and is executed on a set of dedicated compute nodes. SAINT jobs are managed using Torque, an open-source computing resource management system. All SAINT analysis requests are queued and executed on a first-come, first-served basis. The entire infrastructure is currently hosted on FLUX, the university-wide shared high-performance computing service at the University of Michigan. In addition to professional data backup and system management, its allocation-based system allows adding computing nodes to the system if additional computing nodes are needed for running SAINT or other computation-heavy steps that may be added in the future.

The actual data for each experiment ('data'; **Supplementary Fig. 1**), such as the protein/gene accession numbers, the sequences of the identified peptides, peptide probabilities and the spectral counts, are stored in a SQLite database. The attributes used to annotate the experimental conditions (metadata) are stored in a separate MySQL database. The separation of data and metadata is performed for the convenience of developing the web interface, which allows annotation of experiments (management of metadata) directly by data contributors, whereas the processing and management of the data themselves is performed by the database administrator.

So that annotation of data is kept consistent, the attributes and values that describe the experimental conditions are predefined. The corpus of these attributes (and their values) is referred to as the 'controlled vocabularies', or CVs (**Supplementary Table 1**). In addition to the CVs, each experiment deposited in the CRAPome repository is also annotated with a detailed description of the experimental protocol that enables users to obtain additional details about the experiments.

Processing of mass spectrometry data and population of the CRAPome database. Data sets were obtained from the contributing laboratories in the .raw or .mgf file formats. The files were converted to the open mzXML file format and further processed using the X!Tandem/Trans-Proteomic Pipeline (TPP) suite of tools^{36–38}. MS/MS spectra were searched against RefSeq protein sequence database version 47 (ref. 39; *H. sapiens*) or SGD ORF protein sequence database orf_trans.20100105.fasta (*S. cerevisiae*), appended with an equal number of decoy sequences, using X!Tandem⁴⁰ with *k*-score plug-in. For the purposes of simplicity and uniformity, we developed two standard parameter templates for processing using X!Tandem and TPP, which were applied to data generated on low- or high-mass accuracy instruments, respectively. MS/MS spectra were searched using a precursor mass tolerance of 100 p.p.m. (monoisotopic mass) or using -1 to +4 Da (average mass) window for high- and low-mass accuracy instruments, respectively. All other database search parameters were identical: cysteine carbamylation (C + 57.0215) and methionine oxidation (M + 15.9949) were specified as variable modifications. The search results were processed using

PeptideProphet (high-mass accuracy data were analyzed using the high-mass accuracy binning option) and then further processed using ProteinProphet to create protein summary files. For each experiment, all contributing data (multiple gel-band fractions, technical replicates, etc.) were combined to generate a single set of PeptideProphet and ProteinProphet output files (pepXML and protXML files, respectively). One of the submitted data sets¹⁶ consisted of a very large number (300) of negative controls in which proteins were separated using 1D SDS-PAGE. In a fraction of these experiments, only selected bands were analyzed using MS. To avoid the problem of data inconsistency due to missing MS data for a subset of gel fractions, and to reduce the total number of entries in the CRAPome representing this data set, we combined the individual experiments from this data set to generate ten composite experiments (protocol no. 66; experiments CC185–CC194).

To build the CRAPome database, we extracted spectral counts from protXML files using an in house-built software tool. For each protein in the protXML file, peptide-to-spectrum matches with a probability ≥ 0.9 were extracted. The cumulative sum of the spectral assignments for these peptides constituted the spectral count for the corresponding protein. The spectral count was computed for each protein in the output file regardless of whether peptides mapping to a given protein could also map to other proteins. We note that this represents a deviation from the conventional approach of performing stringent false discovery rate (FDR) filtering and removing redundant or inconclusive, i.e., not supported by unique peptides, protein identifications⁴¹. (The results of such stringent filtering are described below; see "Global analysis and reduced gene counts.") The liberal approach for creating protein summaries for each experiment taken here in fact enables a conservative approach for scoring protein interactions. As discussed in ref. 8, it ensures that the spectral counts of proteins from homologous families such as keratins, tubulins and actins are not underestimated owing to the ambiguities related to the identification of shared peptides. Finally, RefSeq protein accession numbers were mapped to official gene identification numbers using Ensembl BioMart tools and were displayed as corresponding gene symbols (entries with NP accession numbers only; proteins with XP numbers and those with NP accession numbers that cannot be mapped to gene symbols are presently not visible in the database). When multiple proteins mapped to the same gene entry, the maximum spectral count among these proteins was selected as the spectral count for that gene. These data provided the basis of the CRAPome accessible online and were used to calculate redundant gene counts shown in **Table 1**.

Quality control. As part of the process of creating the database, the CRAPome administrator performs a quality-control check of the database search results. Experiments containing only a few identifications (fewer than 10 gene symbols with nonzero counts) are removed automatically, and experiments with 10–50 gene symbols are inspected in more detail. Furthermore, all negative-control experiments generated using the same protocol (biological replicates) are inspected for consistency, and inconsistent samples are removed. Last, possible carryover issues are identified and referred to the data depositors for further inspection. From the 402 experiments submitted to the CRAPome, 42 experiments were excluded on the basis of these quality-control steps.

Global analysis and reduced gene counts. To allow a more informative analysis of the contaminant profiles and comparison with other data, we processed all pepXML and protXML files generated as described above using a more conventional set of filtering thresholds. All pepXML files used to generate the CRAPome repository (human data subset, 343 files) were processed together using ProteinProphet to generate a single protein summary file (protXML file). This combined protXML file, as well as the pepXML and protXML files for each individual experiment, were then processed using Abacus⁴² to generate a combined spectral count matrix using default parameters (accepting proteins with at least one peptide having PeptideProphet probability of 0.99 or greater and protein probability as computed by ProteinProphet of 0.9 or greater). Each row in the filtered Abacus file represented a protein group from the combined protXML file, with a single accession number selected among indistinguishable protein entries forming that group. Spectral counts for the representative proteins were extracted from pepXML files for each individual experiment. The FDR for the combined protein list was less than 1% as estimated using decoy counts. The resulting spectral count matrix was used to compute similarity scores to generate the clustergram (see below) and to analyze the global properties of the data such as frequency of identification across the entire data set (Table 1, ‘reduced gene count’).

Gene Ontology (GO) enrichment analysis was performed on the reduced list, and only the top 25% most abundant proteins in each experiment were considered (1,427 genes in total). The analysis was done using the online DAVID tool⁴³, with the analysis restricted to level 3 biological process (BP), molecular function (MF), or cellular component (CC).

To generate the clustergram (Fig. 2b), we first computed experiment-experiment similarity scores using the cosine function from square root-transformed spectral counts (data from protocol no. 66 (ref. 16) were excluded from this analysis; see above). For computing the final clustergram, we required that each experiment had at least two additional experiments with a similarity score of 0.7 or higher. The final clustergram was generated using Cluster 3.0 software⁴⁴, with single-linkage clustering using Pearson correlation (uncentered) as the similarity measure. The clustergram was visualized using TreeView software⁴⁵.

Background contaminant propensity as a function of protein abundance in HEK293 cells. To generate the list of proteins and protein abundances in the HEK293 whole-cell lysate, we used publicly available data taken from ref. 32. Raw mass spectrometry data for this cell line were downloaded from the original publication and processed as described above (see “Global analysis and reduced gene counts”). For each identified protein (representative protein per group; see above) in the filtered Abacus file, the summed spectral count across the four biological replicates was taken as a measure of the protein abundance in the cell line. A global histogram of protein abundances was then generated by binning (Fig. 2a). The background contaminant propensity was then calculated as a fraction of HEK293 cell line-identified proteins in each spectral count bin that were also detected in at least one HEK293 experiment in the CRAPome. For this comparison, we selected CRAPome experiments having the “Cell Line” attribute value “HEK293” only and queried protein accession numbers identified in the HEK293 whole-cell lysate against the

CRAPome HEK293 identified proteins. We then plotted the “fraction in CRAPome” as a function of protein abundance (binned spectral counts).

Data formats. When users query the database to view contaminant profiles for selected proteins of interest (workflow 1), proteins can be referenced using a variety of identifiers: RefSeq protein ID, Ensembl protein ID, NCBI Gene ID, UniProt entry name, UniProt entry ID, HGNC gene symbol (human) or SGD ID (*S. cerevisiae*). All input identifiers are internally mapped to official gene identification numbers using Ensembl Biomart⁴⁶ tools and displayed as corresponding gene HGNC symbols (SGD ID for *S. cerevisiae*). Input data for uploading to the CRAPome for analysis in workflow 3 can be formatted using any of the accession schemes references above. The input file needs to be formatted to contain four columns: “Bait Name,” “AP Name,” “Prey Name,” and “Spectral Count.” Each row in this file lists the spectral count (Spectral Count column) for each protein (referenced in Prey Name column) in purification with a particular bait protein (bait protein/gene identifier is referenced in the Bait Name column). When multiple biological replicates for the same bait are available, they are distinguished using different text strings in the AP Name column (for example, “R1,” “R2,” etc.). The negative-control runs are specified by the text string “CONTROL” in the Bait Name column (and named differently in the AP Name column: for example, “UC1,” “UC2,” etc.).

AP-MS test data. The analytical pipeline is illustrated using two biological replicates of each of the following four baits. RAF1 is a serine/threonine kinase that binds to Ras, several chaperones and 14-3-3 proteins^{47,48}. EIF4A2 is a translation initiation factor that is part of the EIF4F complex, which bridges the mRNA cap structure to the ribosome via the EIF3 complex⁴⁹. WASL (also known as N-WASP) belongs to the Wiskott-Aldrich syndrome (WAS) family of proteins, involved in transduction of signals from receptors on the cell surface to the actin cytoskeleton⁵⁰. Finally, MEPCE, the 7SK snRNA methylphosphate capping enzyme, interacts with numerous transcriptional and RNA-processing proteins⁵¹.

Cloning and expression of EIF4A2, RAF1 and MEPCE has been previously described¹⁵. WASL and ORC2L were amplified by PCR from Mammalian Gene Collection constructs BC052955 and BC014834, respectively, and were cloned into pcDNA5-FRT-Flag (using EcoRI/NotI for WASL and AscI/NotI for ORC2L), and the junctions were sequenced. The primers used were WASL_5'EcoRI, GATCGAATTCATGAGCTCCGTCCAGCAGC; WASL_3'NotI, GATCGCGGCCGCTCAGTCTTCCCACATCATCATC; ORC2L_5'AscI, GATCGGCGGCCAATGAGTAAACCAGAAT TAAAGGAAGAC; ORC2L_3'NotI, GATCGCGGCCGCTCAAG CCTCTTCTTCC. The resulting vectors were stably cotransfected with the FLP-recombinase-expressing vector pOG44 into FLP-In T-REx 293 cells (Invitrogen). Selection of stable transformants (single clones), clonal expansion, induction of protein expression and AP-MS were performed essentially as described in ref. 15 using Flag M2 agarose beads (Sigma). Two biological replicate analyses of each bait were performed, alongside six negative controls (cells expressing the tag alone). All samples were analyzed on an LTQ mass spectrometer coupled to an online C18 reversed-phase column. The detailed protocol is no. 48 in the

CRAPome. The mass spectrometry data were searched using the X! Tandem/TPP/ABACUS pipeline and settings as described in “Global analysis and reduced gene counts.” The filtered Abacus file was formatted for CRAPome as described in “Data formats” using an in-house tool. Data were uploaded to the CRAPome (workflow 3). Two sets of additional controls (set 1 and set 2; see main text) were selected and used alongside the user controls. SAINT and FC scores were generated using different settings (see main text and below). The ORC2L bait was processed in a similar way and uploaded for analysis to the CRAPome separately (it was not used for comparison between SAINT and FC scores shown in Fig. 3). The resulting input data matrices for EIF4A2, RAF1, MEPCE and WASL baits, and the six user controls, as well as for ORC2L and the same user controls, can be downloaded from the CRAPome website.

Interaction scoring: SAINT. SAINT was described in ref. 29. Here the data were analyzed using SAINT options “LowMode = 0, MinFold = 0, Normalize = 1.” In general, SAINT performance varies depending on the choice of options, especially MinFold (requiring a certain minimum fold change as a part of probability calculation) and Normalize (normalization to the total spectral count in each experiment). SAINT runs with the options specified above slightly outperform SAINT results with other options applied to these data (Supplementary Fig. 2). When the bait protein is analyzed in multiple biological replicates, SAINT probabilities computed independently for each bait replicate are averaged, and the average probability (AveP) is reported as the final SAINT score. For in-depth discussion of these options, see ref. 30. The CRAPome also allows alternative specifications for combining biological replicates (for example, geometric mean as a more conservative approach).

SAINT has been shown to perform well when using a sufficient number of matching negative controls (ideally, at least 3–5 controls) showing a high degree of reproducibility. At the same time, SAINT can be sensitive to changes in the spectral count distributions of a given protein in either the controls or the bait samples, and its performance may thus be affected if the bait sample quality is poor or the negative controls are heterogeneous. SAINT is also computationally intensive.

Interaction scoring: fold change. The primary FC score (FC-A, or just FC) can be considered an alternative to SAINT scoring. It is computed for each bait-prey interaction pair (initially separately for each biological replicate of the bait). It is defined as the ratio of the normalized spectral count of protein i in purification with bait j , $T_{i,j}$, to the average normalized spectral count of that protein across the negative controls (user controls or selected CRAPome controls), C_i , calculated as $FC_{i,j} = (T_{i,j} + \alpha)/(C_i + \alpha)$. The normalized spectral counts are computed as $T_{i,j} = SC_{i,j}/N_j$, where the normalization factor is the sum over all proteins identified in the experiment with bait j , $N_j = \sum SC_{i,j}$. Similarly, the counts are normalized in each negative-control experiment $x = 1 \dots n$, $C_{i,x} = SC_{i,x}/N_x$, before the averaged normalized count across all n controls, $C_i = 1/n \sum C_{i,x}$, is computed. A small background factor α is added to prevent division by 0, calculated as $\beta/\text{ave}(N_x)$, where $\text{ave}(N_x)$ is the average normalization factor across all n negative controls. The parameter β is by default set to 1. When the bait protein is analyzed in multiple biological replicates, the FC scores

computed independently for each bait replicate are averaged to arrive at the final FC score.

The secondary, more conservative FC score (FC-B) can be used in addition to SAINT or the primary FC-A score for improved detection of several classes of challenging contaminants. It is computed as described above, except that C_i is computed by averaging the three highest normalized spectral counts across all controls (by default, using the combined set of selected CRAPome controls and the user controls, when available). Furthermore, in the case of biological replicates for the bait protein, the final FC-B score is computed by default as the geometric mean of the FC scores for each replicate.

Comparison to literature data. To rapidly benchmark scoring performance and to provide users with a view of the new data in the context of previously published results, a mapping of the interactions to those deposited in the iRefIndex repository³¹ (currently v.9.0) is provided in the interface. iRefIndex was selected because of its comprehensiveness in the number of interactions annotated (it aggregates data from primary curation databases) and the relative ease of download and data mapping. Each entry from the database is mapped to a pair of genes (interacting proteins) using an in-house mapping tool. Entries identified as “complex” are excluded from this mapping. Owing to uncertain quality of previously reported interactions involving ribosomal proteins, which are among the most common contaminating proteins in AP-MS experiments, we excluded all RPL and RPS proteins from the computation of ROC curves shown in Figure 3.

Access to the database. The CRAPome can be accessed at <http://www.crapome.org/>. No registration is required to access workflows 1 and 2. Registration is required for users to analyze their own data in workflow 3, and registration will enhance the functionality of workflow 2. Registration allows the users to save selected lists of controls (Fig. 1c), to use their previously uploaded data, and to access the results of previously performed SAINT and FC analyses.

36. Keller, A., Nesvizhskii, A.I., Kolker, E. & Aebersold, R. Empirical statistical model to estimate the accuracy of peptide identifications made by MS/MS and database search. *Anal. Chem.* **74**, 5383–5392 (2002).
37. Nesvizhskii, A.I., Keller, A., Kolker, E. & Aebersold, R. A statistical model for identifying proteins by tandem mass spectrometry. *Anal. Chem.* **75**, 4646–4658 (2003).
38. Deutsch, E.W. *et al.* A guided tour of the Trans-Proteomic Pipeline. *Proteomics* **10**, 1150–1159 (2010).
39. Pruitt, K.D., Tatusova, T., Brown, G.R. & Maglott, D.R. NCBI Reference Sequences (RefSeq): current status, new features and genome annotation policy. *Nucleic Acids Res.* **40**, D130–D135 (2012).
40. Craig, R. & Beavis, R.C. TANDEM: matching proteins with tandem mass spectra. *Bioinformatics* **20**, 1466–1467 (2004).
41. Nesvizhskii, A.I. & Aebersold, R. Interpretation of shotgun proteomic data: the protein inference problem. *Mol. Cell. Proteomics* **4**, 1419–1440 (2005).
42. Fermin, D., Basrur, V., Yocum, A.K. & Nesvizhskii, A.I. Abacus: a computational tool for extracting and pre-processing spectral count data for label-free quantitative proteomic analysis. *Proteomics* **11**, 1340–1345 (2011).
43. Huang, D.W., Sherman, B.T. & Lempicki, R.A. Systematic and integrative analysis of large gene lists using DAVID bioinformatics resources. *Nat. Protoc.* **4**, 44–57 (2009).
44. de Hoon, M.J., Imoto, S., Nolan, J. & Miyano, S. Open source clustering software. *Bioinformatics* **20**, 1453–1454 (2004).

45. Page, R.D. TreeView: an application to display phylogenetic trees on personal computers. *Comput. Appl. Biosci.* **12**, 357–358 (1996).
46. Kasprzyk, A. BioMart: driving a paradigm change in biological data management. *Database (Oxford)* **2011**, bar049 (2011).
47. Tzivion, G., Luo, Z. & Avruch, J. A dimeric 14-3-3 protein is an essential cofactor for Raf kinase activity. *Nature* **394**, 88–92 (1998).
48. Wartmann, M. & Davis, R.J. The native structure of the activated Raf protein kinase is a membrane-bound multi-subunit complex. *J. Biol. Chem.* **269**, 6695–6701 (1994).
49. Gingras, A.C., Raught, B. & Sonenberg, N. eIF4 initiation factors: effectors of mRNA recruitment to ribosomes and regulators of translation. *Annu. Rev. Biochem.* **68**, 913–963 (1999).
50. Miki, H., Miura, K. & Takenawa, T. N-WASP, a novel actin-depolymerizing protein, regulates the cortical cytoskeletal rearrangement in a PIP2-dependent manner downstream of tyrosine kinases. *EMBO J.* **15**, 5326–5335 (1996).
51. Jeronimo, C. *et al.* Systematic analysis of the protein interaction network for the human transcription machinery reveals the identity of the 7SK capping enzyme. *Mol. Cell* **27**, 262–274 (2007).